

## THE INFLUENCE OF TIN ON PRECIPITATION PROCESSES AND MECHANICAL PROPERTIES OF A MACHINABLE LEAD-FREE Al-Cu ALLOY

IVANA STULÍKOVÁ<sup>1\*</sup>, BOHUMIL SMOLA<sup>1</sup>, MIROSLAV CIESLAR<sup>1</sup>,  
MICHAL HÁJEK<sup>1</sup>, JITKA PELCOVÁ<sup>1</sup>, OXANA MELIKHOVA<sup>1</sup>,  
JIŘÍ FALTUS<sup>2</sup>

The replacement of lead by tin in Al-Cu-Bi alloy leads to differences in the early stages of decomposition processes. While Al-Cu-Bi-Pb decomposes similarly to Al-Cu alloy, the presence of Sn suppresses the formation of Cu-rich GP zones. Instead, a modulated structure develops and transforms directly into  $\alpha$ -matrix and fine dispersed  $\theta'$  (metastable,  $\text{Al}_2\text{Cu}$ ) plates oriented along  $\{100\}$  planes of  $\alpha$ -matrix. We attribute it to the high tin-vacancy binding energy and the formation of tin-vacancy agglomerates. The influence of small tensile plastic deformation at room temperature preceding the isochronal annealing of solution treated alloys on precipitation is more pronounced in Al-Cu-Bi-Pb than in Al-Cu-Bi-Sn. The fine dispersed rationally oriented  $\theta'$  plates in Al-Cu-Bi-Sn cause a high degree of hardening. The hardness values and the increments of flow stress due to dislocation looping of precipitates, calculated from observed precipitate volume fraction and their aspect ratio, are in a good agreement.

## VLIV CÍNU NA PRECIPITAČNÍ PROCESY A MECHANICKÉ VLASTNOSTI OBROBITELNÉ BEZOLOVNATÉ SLITINY Al-Cu

Náhrada olova cínem ve slitině Al-Cu-Bi vede k odlišnostem v raných stádiích rozpadu přesyceného tuhého roztoku. Zatímco rozpad v Al-Cu-Bi-Pb je podobný jako v Al-Cu, cín potlačuje tvorbu GP zón bohatých na Cu. Namísto toho vzniká modulovaná struktura, ze které se přímo tvoří jemná disperze destiček fáze  $\theta'$  (metastabilní,  $\text{Al}_2\text{Cu}$ ) ležících v rovinách  $\{100\}$   $\alpha$ -matrice. Tento jev připisujeme vysoké vazebné energii mezi cínem a vakancí a tvorbě jejich aglomerátů. Malá plastická deformace tahem při pokojové teplotě zařazená mezi rozpouštěcí žhání a izochronní žhání ovlivňuje více precipitaci v Al-Cu-Bi-Pb než v Al-Cu-Bi-Sn. Jemná disperze uspořádaných destiček  $\theta'$  je příčinou velmi dobrého vytvrzení slitiny Al-Cu-Bi-Sn. Příspěvky napětí vyplývající z Orowanova mechanismu překonávání precipitátů dislokacemi, které byly spočítány na základě pozorovaných

<sup>1</sup> Faculty of Mathematics and Physics, Charles University, Ke Karlovu 5, 121 16 Prague 2, Czech Republic

<sup>2</sup> Research Institute of Metals, Panenské Břežany, 250 70 Odolena Voda, Czech Republic

\* corresponding author, e-mail: [ivana.stulikova@mff.cuni.cz](mailto:ivana.stulikova@mff.cuni.cz)

objemových podílů a rozměrů destiček, jsou v dobré shodě s měřenými hodnotami tvrdosti.

**Key words:** Al-Cu-Bi-Sn, Al-Cu-Bi-Pb, precipitation processes, hardness, modified Orowan equation

## 1. Introduction

Machinability problems like chip removal and quality of machined surface can reduce productivity. The presence of a low melting point eutectic constituent in an aluminium alloy is the successful way to form small chips. Conventional Al-Cu alloys were designed with the addition of a Pb-Bi eutectic. These low melting point additions are usually fine and dispersed throughout the material. The elements used have inconsiderable solubility in the matrix. It is believed that the temperature in the vicinity of the dispersoids rises near to the melting temperature of the dispersoids during a machining operation. This leads to the loss of ductility and strength and to the formation of short, discontinuous chips. However, the use of these alloys is being discouraged due to environmental problems with Pb. The substitution of Pb with Sn has been proposed [1] to solve this problem.

It was shown that an addition of Pb and Bi to Al-Cu alloy does not change its precipitation sequence [2] and this can be written schematically as [3]:

SSS  $\rightarrow$  GP zones I  $\rightarrow$  GP zones II  $\rightarrow$  semicoherent metastable  $\theta'$   $\rightarrow$  incoherent stable  $\theta$  ( $\text{Al}_2\text{Cu}$ ).

The precipitation sequence can be changed by substituting Pb with Sn. Hardy showed that trace additions of Cd, In or Sn gave accelerated and higher hardening in Al-Cu alloys [4, 5]. It seems that nucleation by traces of Sn is specific to  $\theta'$  phase in Al-Cu alloys so that the part of the precipitation sequence GP zones I  $\rightarrow$  GP zones II is restricted and eliminated above 150°C [6]. The effects of trace additions of Cd, In or Sn on the nucleation of  $\theta'$  phase in Al-Cu alloys were attributed to a lowering of the interfacial energy of  $\theta'$  nuclei by the trace elements [7] or to nucleation at prior formed Cd, In or Sn precipitates [8]. These precipitates strongly bind vacancies that cannot assist the diffusion of Cu in Al. The formation of GP zones is therefore suppressed and the decomposition of supersaturated solid solution starts at higher temperatures directly by the formation of  $\theta'$  phase. According to the recent review [6], both mechanisms are possible, depending on the conditions of thermal treatment.

The aim of the work was to investigate the precipitation processes in a new Al-Cu-Sn-Bi alloy containing higher than a trace content of Sn in the temperature range up to 500°C and to study the effect of these processes on mechanical properties. The commercial Al-Cu-Pb-Bi alloy was used as a reference material.

## 2. Experimental details

Two investigated alloys were prepared in ALUSUISSE Děčín (now ALCAN), Czech Republic. The actual composition was determined by atomic absorption spectroscopy and is given in Table 1. Both alloys were extruded, solution treated, stretched at room temperature, and artificially aged. These procedures followed the standards for commercial alloys. Parameters of the thermomechanical treatment are given in Table 2.

Table 1. Alloys composition in wt.%

	Cu	Pb	Sn	Bi	Fe	Si	Zn	Mg	Mn	Ti	Sb
Al-Cu-Bi-Pb	5.62	0.51	<0.005	0.51	0.3	0.13	0.027	0.0087	0.007	0.005	0.005
Al-Cu-Bi-Sn	4.6	0.014	0.36	0.59	0.16	0.06	0.024	0.0066	0.0071	0.0048	0.002

Table 2. Procedures in the preparation of alloys

	Solution treatment followed by water quenching	Stretching at room temperature	Artificial ageing
Al-Cu-Bi-Pb	515 °C/1 h	4 %	160 °C/12 h
Al-Cu-Bi-Sn	530 °C/1 h	8 %	140 °C/10 h

The isochronal annealing response of relative electrical resistivity changes was determined in the range 20–500 °C at specimens once more solution heat treated at 530 °C for 30 min and subsequently water quenched. Isochronal annealing was carried out in steps of 20 K/20 min or 30 K/30 min or 50 K/50 min followed by quenching. This treatment was performed in a stirred oil bath up to 240 °C or in a furnace with argon protective atmosphere at higher temperatures. The H-shaped specimens were used for resistivity measurements in liquid nitrogen at 77 K after each heating step. Relative electrical resistivity changes  $\Delta\rho/\rho$  were obtained within an accuracy of  $10^{-4}$ . The resistivity was measured by means of the dc four-point method with a dummy specimen in series. The influence of parasitic thermoelectromotive force was suppressed by current reversal.

The thermal stability of mechanical properties was measured by Vickers hardness HV30 at room temperature. The same isochronal annealing procedure as for the resistivity measurements was used.

The evolution of microstructure was followed using transmission electron microscopy (TEM) and electron diffraction (ED) (JEOL JEM 2000FX electron microscope). The phase composition was determined using Link AN 10000 microanalyser. The specimens prepared for TEM were thermally treated using the same isochronal annealing procedure as for electrical resistivity and hardness measurements.

To prevent any problems with the natural ageing, the specimens were kept in liquid nitrogen between measurement and following annealing.

### 3. Experimental results and their discussion

Fig. 1 shows the relative resistivity changes as a function of annealing temperature for both alloys investigated. It is clear that the first decomposition stages of the supersaturated solid solution are different in both alloys. The initial resistivity increase in Al-Cu-Bi-Pb alloy is followed by a slight decrease in the range 80–200 °C, while similar effects are finished already at 160 °C in Al-Cu-Bi-Sn alloy. The main resistivity drop is situated between 220–320 °C in Al-Cu-Bi-Pb alloy while the beginning of this stage is shifted to 160 °C in Al-Cu-Bi-Sn alloy. Relative resistivity changes due to the annealing are very similar in both alloys above 320 °C. Small tensile plastic deformation at room temperature (3 or 6 %) inserted after the repeated solution heat treatment affects the isochronal annealing resistivity curve of Al-Cu-Bi-Sn alloy only slightly, while the first increase of resistivity is suppressed in Al-Cu-Bi-Pb alloy and the beginning of the main stage is shifted to 180 °C (Fig. 2) [9].

The resistivity annealing curve of Al-Cu-Bi-Pb alloy reflects the precipitation effects usually observed in Al-Cu alloy [10]. The slight resistivity increase and the slight decrease below 200 °C are both due to the formation and growth of GPI and GPII zones. The drop of resistivity between 220 °C and 320 °C is attributed to the transformation of GP zones into the semicoherent metastable  $\theta'$  ( $\text{Al}_2\text{Cu}$ ) precipitates and their further coarsening. Above 320 °C, the transformation of metastable  $\theta'$  into the stable  $\theta$  ( $\text{Al}_2\text{Cu}$ ) particles, their growth, coarsening and redissolution

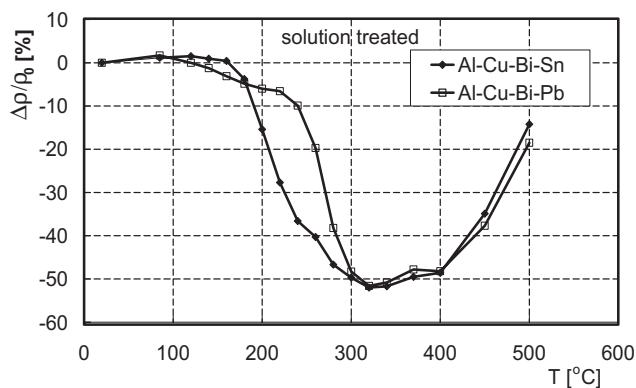


Fig. 1. Relative resistivity changes measured at 77 K due to isochronal annealing.  $\rho_0$  is the initial resistivity value in solution treated state.

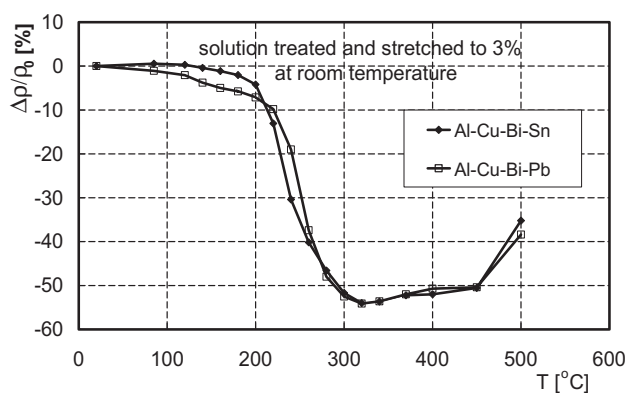


Fig. 2. Relative resistivity changes measured at 77 K due to isochronal annealing.  $\rho_0$  is the initial resistivity value of solution treated state and pre-strained state. The tensile deformation of 3 % was performed at room temperature.

into the matrix manifest themselves as the resistivity increase. The partial suppression of early precipitation stages due to the pre-straining at room temperature is most probably caused by an interaction of Cu atoms with dislocations and by the deformation-induced reduction of free vacancy concentration. The formation of GP zones is thus suppressed and  $\theta'$  precipitates form directly from the supersaturated solid solution heterogeneously at dislocations at lower temperature.

A detailed investigation of the microstructure evolution of solution treated and annealed Al-Cu-Bi-Sn alloy [11] revealed rare insulated islands of a modulated structure in the solution treated material. This modulated structure was observed in the entire specimen volume after annealing up to 160 °C. GP zones were observed neither in the solution treated specimens nor in the annealed condition. No evidence for Sn precipitates was obtained in the initial state, but very weak diffraction spots that can be indexed in accordance with the  $\beta$ -Sn phase confirm the presence of very small particles of this phase in specimens annealed up to 160 °C and 180 °C. The clusters of Sn atoms in the pre-precipitation stage of the  $\beta$ -Sn phase precipitation are most probably surrounded by quenched-in vacancies [12] due to the high tin-vacancy binding energy. This suggestion is supported by the measurements of the annealing curve of positron lifetime performed for the same alloy [13]. The lack of free vacancies inhibits the formation of GP zones and stimulates the development of a modulated structure.

The modulated structure in Al-Cu-Bi-Sn alloy is unstable above 160 °C and transforms directly into a fine dispersion of  $\theta'$  ( $\text{Al}_2\text{Cu}$ ) plates in the  $\alpha$  matrix. These plates are oriented along  $\{100\}$  planes of  $\alpha$  matrix (see Fig. 3) and they precipitate

heterogeneously on  $\beta$ -Sn particles. Their dimensions and volume fraction change in the temperature range 180–320 °C. Above 320 °C, the transformation of  $\theta'$  phase into the stable  $\theta$  phase was observed.

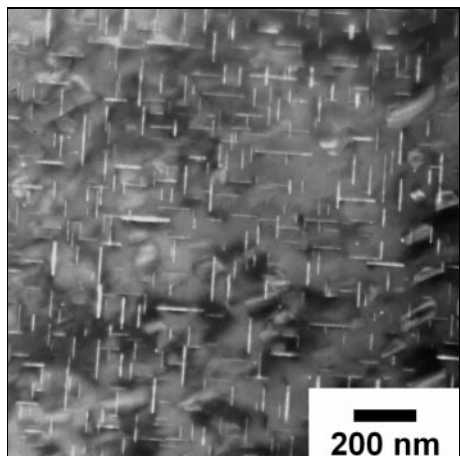


Fig. 3. Transmission electron micrograph of the Al-Cu-Bi-Sn alloy annealed isochronally up to 240 °C. Dark-field image of the  $\theta'$  ( $\text{Al}_2\text{Cu}$ ) phase near the [001] matrix zone axis.

The influence of created precipitates on mechanical properties was studied as the hardness HV30 response to isochronal annealing of solution treated Al-Cu-Bi-Pb and Al-Cu-Bi-Sn alloys (Fig. 4). It is evident that the age hardening in Al-Cu-Bi-Sn alloy is most pronounced in temperature range 200–260 °C and it also reflects the differences in the precipitation sequences of both alloys. The formation and growth of GP zones (160–220 °C) have an analogous effect on hardening as following formation and growth of  $\theta'$  ( $\text{Al}_2\text{Cu}$ ) phase (220–320 °C) in Al-Cu-Bi-Pb alloy. However in the Al-Cu-Bi-Sn alloy, the direct formation of  $\theta'$  precipitates in a dense dispersion between 160 °C and 200 °C raises the hardness HV30 to more than twice that of the solution treated state.

It is well known that plate-shaped precipitates with rational crystallographic

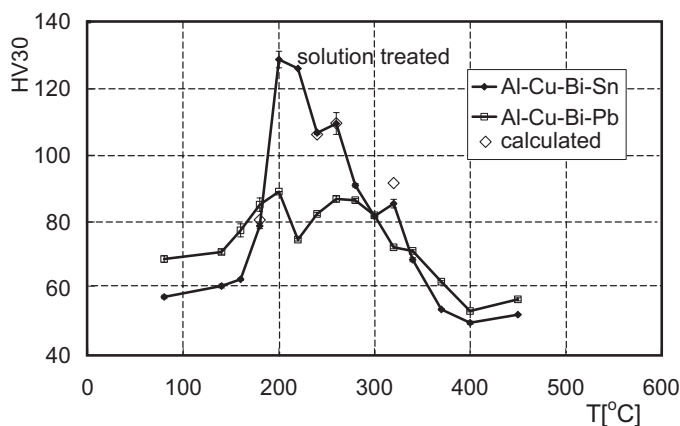


Fig. 4. Hardness HV30 response on isochronal annealing of solution treated alloys.

habit planes and large aspect ratios are frequently associated with high tensile strength. Appropriate versions of the Orowan equation [14] have been developed for aluminium alloys containing rationally oriented  $\{111\}_\alpha$  and  $\{100\}_\alpha$  precipitate plates or  $\langle 100 \rangle_\alpha$  precipitate rods. For aluminium alloys containing  $\{100\}_\alpha$  precipitate plates the increment in critical resolved shear stress (CRSS) due to dispersion hardening  $\Delta\tau_0$  can be written as [15]

$$\Delta\tau_0 = \left\{ \frac{Gb}{2\pi\sqrt{1-\nu}} \right\} \frac{1}{\left( 0.931\sqrt{\frac{0.306\pi dt}{f}} - \frac{\pi d}{8} - 1.061t \right)} \ln\left(\frac{1.225t}{b}\right), \quad (1)$$

where  $G$  is the shear modulus of the matrix,  $b$  is the Burgers vector,  $\nu$  is the Poisson's ratio,  $f$  is the volume fraction,  $d$  is the diameter of plate, and  $t$  is the plate thickness.

The accuracy of volume fraction determination is relatively low due to the uncertainty in the foil thickness measurements. Nevertheless, the clear increase of volume fraction with increasing annealing temperature is evident and agrees with the observed resistivity decrease caused by the matrix purification (Fig. 1). Calculated CRSS increments (Table 3) cannot be directly compared to the measured hardness increments (Fig. 4). The combination of different hardening mechanisms in the resulting flow stress or hardness is not exactly known but it is obviously more complicated than a simple linear addition.

The linear relation between yield stress  $R_p0.2$  and hardness HV30 was found for the alloy studied (Fig. 5) [19].

The slope of this dependence is very near to the value of Taylor factor for f.c.c. metals, namely 3.06 [3]. Within the accuracy of CRSS evaluation the quadratic combination of calculated  $\Delta\tau_0$  values (Table 3) with initial hardness value (HV30  $\sim 58$ ) agree well with the hardness measured (Fig. 4). We are convinced that this agreement is not accidental. A quadratic addition of the flow stress contributions of different hardening processes that are simultaneously effective is regarded as the most probable one [20].

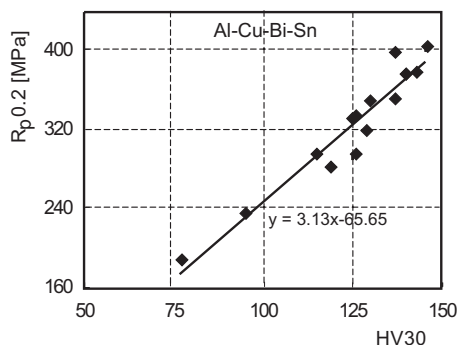


Fig. 5. Linear relationship between HV30 and  $R_p0.2$  for AlCuBiSn alloy after various thermal treatments.

Table 3. Precipitate parameters of AlCuBiSn alloy and corresponding CRSS increments after equation (1) at various annealing temperatures

Annealing temperature [°C]	Volume fraction	Plate diameter [nm]	Plate thickness [nm]	$\Delta\tau_0$ [MPa]
180	$(1.00 \pm 0.25) \times 10^{-2}$	40	3.5	$56 \pm 15$
240	$(2.8 \pm 0.7) \times 10^{-2}$	64	4	$89 \pm 25$
260	$(4.5 \pm 1.1) \times 10^{-2}$	96	7	$93 \pm 26$
320	$(5.0 \pm 1.2) \times 10^{-2}$	159	11.5	$71 \pm 20$

#### 4. Conclusions

1. While the addition of Pb and Bi does not change the decomposition sequence of Al-Cu alloy, 0.36 wt.% Sn in an Al-Cu-Bi alloy causes significant deviations from this sequence. Cu-rich GP zones are not formed in the Al-Cu-Bi-Sn alloy, probably due to the high tin-vacancy binding energy and the formation of tin-vacancy agglomerates. The decomposition starts spinodally with the formation of a modulated structure. Above 160 °C it transforms directly into an  $\alpha$ -matrix and fine dispersed  $\theta'$  ( $\text{Al}_2\text{Cu}$ ) plates oriented along  $\{100\}$  planes of  $\alpha$ -matrix. Volume fraction and dimensions of the plates develop in temperature range 180–320 °C. Above 320 °C, the transformation of metastable  $\theta'$  into the stable  $\theta$  ( $\text{Al}_2\text{Cu}$ ) particles, their growth, coarsening and redissolution into the matrix was observed to be similar to Al-Cu and Al-Cu-Bi-Pb alloy.

1. A little tensile deformation at room temperature after the repeated solution heat treatment suppresses the formation of GP zones in Al-Cu-Bi-Pb alloy and  $\theta'$  precipitates form directly from the supersaturated solid solution more frequently. This pre-straining affects the precipitation processes in Al-Cu-Bi-Sn alloy only slightly.

3. Compared to Al-Cu-Bi-Pb alloy, the dense distribution of  $\theta'$  ( $\text{Al}_2\text{Cu}$ ) precipitates in Al-Cu-Bi-Sn formed during the isochronal annealing causes very pronounced hardening in the temperature range 200–260 °C. The flow stress increments calculated using modified Orowan equation and experimentally determined parameters of precipitates explain well the hardness development during isochronal annealing.

#### Acknowledgements

The support by the Grant Agency of Czech Republic in the frame of the project No. 106/00/1047 and by the Research Project MSM 113200002 of the Ministry of Education, Czech Republic is gratefully acknowledged.

The authors would like to compliment Prof. Z. Trojanová on her 60<sup>th</sup> birthday.

## REFERENCES

- [1] FALTUS, J.—PLAČEK, K.: Aluminium alloy with good machinability. Patent CZ 262896, Priority: 09.09.1996.
- [2] HARDY, H. K.: J. Inst. Met., 79, 1950–51, p. 169.
- [3] HAASEN, P.: Physical Metallurgy. Cambridge, Cambridge Univ. Press 1978.
- [4] HARDY, H. K.: J. Inst. Met., 80, 1951–52, p. 483.
- [5] HARDY, H. K.: J. Inst. Met., 82, 1953–54, p. 236.
- [6] SILCOCK, J. M.—FLOWER, H. M.: Scripta Mater., 46, 2002, p. 389.
- [7] SILCOCK, J. M.—HEAL, T. J.—HARDY, H. K.: J. Inst. Met., 84, 1954–55, p. 23.
- [8] RINGER, S. P.—HONO, T.—SAKURAI, K.: Met. Mat. Trans. A, 26A, 1995, p. 2207.
- [9] VOSTRÝ, P.—STULÍKOVÁ, I.—PELCOVÁ, J.—HÁJEK, M.—CIESLAR, M.—FALTUS, J.: In: Difuze a termodynamika materiálů. Ústav fyziky materiálů AV ČR, Brno 1998, p. 113.
- [10] ČADA, P.—CIESLAR, M.—VOSTRÝ, P.—BEČVÁŘ, F.—NOVOTNÝ, I.—PROCHÁZKA, I.: Acta Physica Polonica, A88, 1995, p. 111.
- [11] CIESLAR, M.—HÁJEK, M.—PELCOVÁ, J.—STULÍKOVÁ, I.—VOSTRÝ, P.: Alum. Trans., 2, 2000, p. 277.
- [12] SZELES, C.—SÜVEGH, K.—HOMONNAY, Z.—VÉRTES, A.: Phys. stat. sol. (a), 103, 1987, p. 397.
- [13] MELIKHOVA, O.—PROCHÁZKA, I.—VOSTRÝ, P.—STULÍKOVÁ, I.—CIESLAR M.—FALTUS, J.: In: Difuze a termodynamika materiálů. Brno, Ústav fyziky materiálů AV ČR 1998, p. 121.
- [14] OROWAN, E.: Symposium on Internal Stresses in Metals and Alloys. London, Institute of Metals 1948, p. 451.
- [15] NIE, J. F.—MUDDLE, B. C.—POLMEAR, I. J.: Mater. Sci. Forum, 217–222, 1996, p. 1257.
- [16] NIE, J. F.—MUDDLE, B. C.: Mat. Sci. Eng. A, 319–321, 2001, p. 448.
- [17] RUSSELL, K. C.—ASHBY, M. A.: Acta Metall., 18, 1970, p. 891.
- [18] MERLE, P.—FOUQUET, F.—MERLIN, J.—GOBIN, P. F.: Acta Metall., 27, 1979, p. 327.
- [19] FALTUS, J.: Research Report 02. Panenské Břežany, VÚK 1996.
- [20] BROWN, L. M.—HAM, R. K.: Dislocation-Particle Interactions. In: Strengthening Methods in Crystals. Eds.: Kelly, A., Nicholson, R. B. London, Applied Science Publishers Ltd. 1971, p. 9.

Received: 31.5.2002